RESEARCH PAPER

ANALYSIS OF FOREST VEGETATION CHANGES IN VIETNAM'S CENTRAL HIGHLANDS AND SOUTHEAST REGIONS USING REMOTE SENSING AND MACHINE LEARNING

Dung Trung Ngo[1*], Duy Dinh Ba[1], Hieu Huu Viet Nguyen[2]
[1]Joint Vietnam-Russia Tropical Science and Technology Research Center, № 63, Nguyen Van Huyen Str., Hanoi, 100000, Vietnam
[2]Forest Inventory and Planning Institute (FIPI), Ngoc Hoi Str., Hanoi, 100000, Vietnam
***Corresponding author:** ngotrungdung@gmail.com
Received: July 22nd 2025 / Accepted: March 25th 2026 / Published: June 30th 2026
https://doi.org/10.24057/2071-9388-2026-4177

ABSTRACT. Forest vegetation is pivotal for maintaining ecological equilibrium and providing essential ecosystem services, yet faces persistent decline, particularly in ecologically sensitive regions like Vietnam's Central Highlands and Southeast. This study aimed to assess the status and dynamics of forest vegetation across these regions from 2016 to 2024, providing a scientific foundation for sustainable forest management. Using Sentinel-2 imagery (10–20 m resolution), GIS, and a Random Forest classifier, we mapped 21 vegetation classes and assessed forest change in Vietnam's Central Highlands and Southeast regions for 2016–2024. The classifier achieved strong performance (mean precision = 0.81, recall = 0.78, F1 = 0.79). Results indicate a net decline in natural forest area (e.g., Rich evergreen broadleaf forest decreased by 2,166.5 ha; Medium coniferous forest decreased by 1,776.8 ha), while "Other lands" increased by 10,232.5 ha and grasslands/shrub/regenerated trees declined by 10,037 ha, reflecting substantial land-use conversion pressures. The study's novelty lies in a refined training-sample collection protocol and systematic hyperparameter optimization tailored to highly heterogeneous tropical vegetation and complex terrain, improving classification reliability for large, fragmented landscapes. These quantitative findings provide actionable evidence to support targeted forest management and land-use change mitigation measures. Urgent implementation of sustainable forest management practices and robust biodiversity conservation measures is imperative to protect these valuable forest ecosystems for future generations.

KEYWORDS: tropical forest, Sentinel-2, Random Forest, mapping, forest management, land-use change

CITATION: Dung Trung Ngo, Duy Dinh Ba, Hieu Huu Viet Nguyen (2026). Analysis Of Forest Vegetation Changes In Vietnam's Central Highlands And Southeast Regions Using Remote Sensing And Machine Learning. Geography, Environment, Sustainability, 2 (19), 67-83
https://doi.org/10.24057/2071-9388-2026-4177

ACKNOWLEDGEMENTS: This research was supported by project ST.Đ1.04/25 "A study on the determination and simulation of net ecosystem production in representative forest ecosystems of the Central Highlands and Southeastern Vietnam using integrated statistical, dynamic, and machine-learning approaches". Funding was provided by the Joint Vietnam-Russia Tropical Science and Technology Research Center.

Conflict of interests: The authors reported no potential conflict of interests.

INTRODUCTION

Tropical rainforest vegetation is a cornerstone of global ecosystems, harboring approximately 50% of the planet's biodiversity and playing an essential role in climate regulation, ecological balance, water resource protection, and climate change mitigation (Denslow 1987, Ostendorf et al. 2001, Ghazoul et al. 2010). Despite covering approximately 11% of the Earth's land surface, tropical rainforests are disproportionately impacted by economic development, resource exploitation, deforestation, and climate change (Amelung et al. 1992, Ogboi 2001, Wan Mahari et al. 2020). Deforestation rates have accelerated in recent decades, driven by increasing demand for timber, agricultural land, and urbanization (Kumar et al. 2022). Reports from the Food and Agriculture Organization (FAO) of the United Nations indicate an average annual global forest loss of approximately 10 million hectares, with a significant portion concentrated in tropical regions, including the Amazon (Binswanger 1991), the Congo Basin (Aquilas et al. 2022), and Southeast Asia (Turner et al. 2023).

Vietnam's Central Highlands and Southeast regions present a distinct combination of basalt-derived fertile soils, pronounced elevation gradients (with Central Highlands plateaus typically ~800–1,000 m), and a tropical monsoon climate (annual rainfall ~1,800–2,500 mm). These environmental gradients drive a mosaic of forest types — including evergreen broadleaf, deciduous dipterocarp, mixed broadleaf–conifer, bamboo stands, and coastal mangroves — and create complex terrain and phenology-induced spectral variability that complicates remote sensing classification. Additionally, forest ecosystems in the Central Highlands and Southeast regions of Vietnam are subject to considerable pressure from illegal logging activities, forest fires, and the impacts of climate change, which threaten both biodiversity and ecosystem services (Tai et al. 2021, Dinh et al. 2023). Recent years have witnessed a growing application of satellite imagery, particularly Sentinel-2 data, for vegetation cover monitoring in this region (Nguyen et al. 2020, Huong et al. 2021). Results indicate that Sentinel-2 imagery offers superior classification accuracy, especially for distinguishing evergreen, semi-evergreen, and agricultural lands in mountainous terrain, primarily due to its fine spatial resolution (Thi Hoai et al. 2025). Furthermore, the integration of Sentinel-2 satellite data with Random Forest (RF) models has demonstrated advantages in tracking dynamic changes across various land cover types within the Central Highlands and Southeast regions of Vietnam (Do et al. 2025). These works demonstrate improved class separability at finer spatial scales but are often constrained by limited geographic extent, single-year analyses, or limited adaptation to topographic illumination effects. Few region-scale, multi-temporal assessments explicitly refine training-sample strategies and hyperparameter tuning to address spectral confusion and mixed-pixel problems across the heterogeneous, mountainous landscapes of the study area.

Faced with the growing need for continuous and comprehensive forest monitoring, traditional field-based methods are increasingly challenged by limitations in temporal frequency, spatial extent, and cost-effectiveness (Schnell et al. 2015). Consequently, modern remote sensing technologies are recognized for their superior capabilities in forest resource management (Hudak et al. 2009, Lechner et al. 2020, Ngo et al. 2024). Satellite-based platforms, such as Landsat (Raši et al. 2011), Sentinel (Erinjery et al. 2018), and high-resolution commercial systems such as WorldView (Ferreira et al. 2021), and RapidEye (Gärtner et al. 2016), provide access to spatially explicit data at appropriate temporal resolutions, enabling near real-time or periodic monitoring of vegetation dynamics. These satellite images provide a wealth of information, including reflectance spectra, spatial resolution, and temporal resolution, facilitating the discrimination of vegetation types and the identification of deforestation, fire disturbances, and illegal logging activities (Dennis et al. 2005, Matricardi et al. 2010, Mujetahid et al. 2023). Furthermore, geographic information system (GIS) technologies enable the integration, processing, and analysis of spatial data to create zoning maps and classification models and simulate trends in forest changes (Pijanowski et al. 2002, Reddy et al. 2017). GIS plays a central role in combining remote sensing data with ancillary information such as ground truth data, field samples, and climate data, thereby facilitating more accurate assessments of forest status and vegetation dynamics within the study area (Weiers et al. 2004, Karan et al. 2016). The integration of remote sensing and GIS with machine learning techniques is emerging as a powerful approach to automating and enhancing forest monitoring capabilities, enabling accurate classification, change detection, and prediction of future forest conditions.

Machine learning techniques have revolutionized environmental monitoring, particularly in the classification and detection of forest change (Himeur et al. 2022, Yun et al. 2024). Algorithms such as RF, support vector machines (SVMs), and convolutional neural networks (CNNs) demonstrate robust capacity for processing large volumes of image data, enabling the identification of characteristic spectral and spatial patterns associated with diverse vegetation types and land cover classes (Sothe et al. 2020, Sothe et al. 2020, Saim et al. 2025). These algorithms, through self-learning and model optimization, often yield higher classification accuracies than traditional methods do, minimizing classification errors and providing more precise predictive capabilities for assessing future change trends (Wang et al. 2025). Furthermore, the integration of satellite data services and cloud-based platforms, such as Google Earth Engine, has significantly reduced technical and logistical barriers, facilitating efficient access, processing, and analysis of large geospatial datasets for continuous monitoring, real-time mapping, and large-scale predictive modeling in support of sustainable forest resource management (Koskinen et al. 2019, Phalke et al. 2020, Jahromi et al. 2021). This combination of remote sensing, GIS, and machine learning offers a potentially scalable, cost-effective, and synoptic approach for monitoring forest resources across expansive and heterogeneous landscapes. While recent studies have primarily focused on smaller, specific areas, our research distinctly addresses the Central Highlands and Southeast regions. This area, characterized by unique ecological transitions and significant development pressures, has seen limited comprehensive, multi-temporal assessments utilizing Sentinel-2 data and RF models. In this study, we introduce a refined methodology for training sample collection and parameter optimization specifically tailored to the highly heterogeneous vegetation structures and complex terrain of these particular regions. This approach meticulously addresses challenges such as spectral confusion and inter-class variability often encountered in such diverse landscapes.

In Vietnam, particularly within the Central Highlands and Southeast regions, the application of remote sensing, GIS, and machine learning for forest monitoring remains underexplored. Specifically, there is a need for methodologies that closely integrate machine learning algorithms with remote sensing and GIS data to improve the efficiency and accuracy of classifying and forecasting vegetation changes under the diverse and complex terrain conditions characteristic of this region. Therefore, the objectives of this study are to (i) develop and validate a Random Forest classification framework tailored to the Central Highlands and Southeast using Sentinel-2 spectral bands, vegetation indices, and terrain variables; (ii) produce multi-temporal vegetation maps for 2016, 2020, 2021, and 2024 and assess classification accuracy; and (iii) quantify spatial–temporal transitions among key forest and non-forest classes to inform targeted forest management and land-use change mitigation. This study advances the regional remote sensing literature by (1) integrating multi-year Sentinel-2 MSI (2016–2024) with Random Forest classification across the full Central Highlands and Southeast regions, (2) implementing a refined protocol for stratified training-sample collection and systematic hyperparameter optimization to adapt the RF model to mountainous terrain and fragmented vegetation, and (3) delivering class-level area-change quantification for 21 vegetation/land-cover types aligned with national inventory cycles — thereby producing spatially explicit, policy-relevant evidence at a regional scale.

MATERIALS AND METHODS

Study area

The study area encompasses the Central Highlands and Southeast regions of Vietnam (Fig. 1). According to a 2025 report by the Vietnamese Ministry of Agriculture and Environment, the total area of the study region is approximately 78,000 km^2. Of this, the Central Highlands region has a total forest area of over 2.59 million hectares with a forest cover rate of 46.34%, making it a region with a large forest area. The Southeast region has a significantly smaller forest area, approximately 479,730 hectares, with a forest cover rate of 19.6%. The topography is characterized by a diverse mosaic of features, ranging from layered plateaus with average elevations of 800 to 1,000 m in the Central Highlands to coastal plains in the Southeast (Shinjo et al. 2024). These regions were specifically chosen for their ecological importance, showcasing diverse and unique forest ecosystems. Additionally, they play a crucial role in national development, which adds significant pressure on natural resources.

The regional climate is classified as a tropical monsoon regime, with distinct wet (May–October) and dry (November–April) seasons. The average annual rainfall ranges from 1,800 mm to 2,500 mm, with precipitation being primarily concentrated during the wet season. The mean annual temperature is approximately 24°C to 27°C, with minimal seasonal variation (Vu et al. 2015, Nguyen Duc et al. 2019). The soil types in this region are diverse, with major classifications including ferralsols, greyzems, fluvisols, and arenosols. Ferralsols, derived from basaltic parent material, cover a substantial portion of the Central Highlands and are distinguished by their porosity, nutrient richness, and suitability for the cultivation of long-term industrial crops and natural forests (Cramb et al. 2004, Van Minh et al. 2020, Nguyen et al. 2025).

The forest vegetation in the Central Highlands and Southeast region is highly diverse and comprises various forest types, such as tropical evergreen closed forests, deciduous dipterocarp forests, mixed broadleaf and coniferous forests, and coastal mangrove forests (Lung et al. 2011, Luong et al. 2015). These natural forest ecosystems play a vital role in biodiversity conservation, water resource regulation, and watershed protection. However, the area of natural forests is decreasing due to logging activities, land use conversion, and agricultural expansion.

The Central Highlands and Southeast regions of Vietnam play a crucial ecological and economic role, providing important water resources, biodiversity, special-use forests, and protective forests. They also have distinct topographic and soil characteristics that make monitoring mountainous forests and industrial plantations challenging, particularly due to elevation changes and basalt soils. Additionally, this region is under significant pressure from land-use changes, including the expansion of industrial crops, agriculture, urbanization, and logging. As a result, there is a need for a regional-scale assessment of land cover changes to support effective management and policy-making.

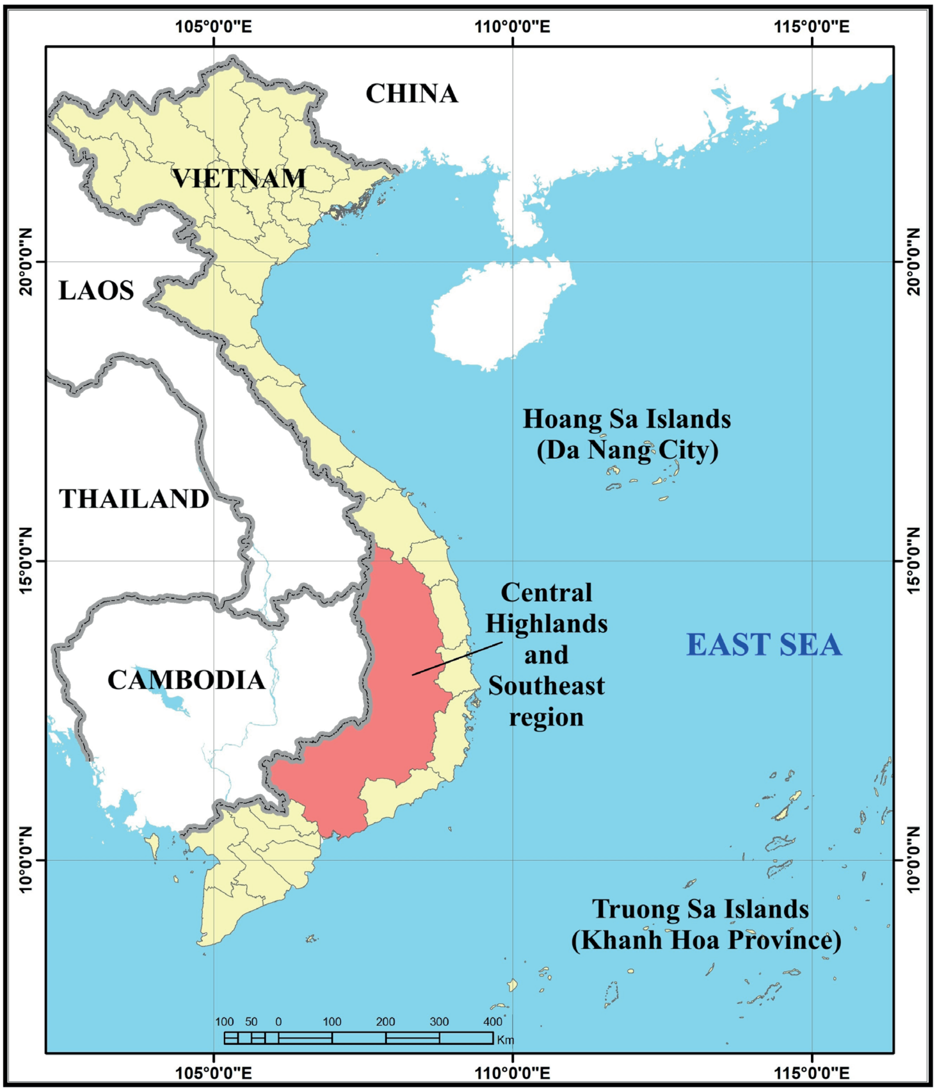

Fig. 1. Locations of the Central Highlands and Southeast Region, Vietnam

Data

Remote sensing data

This study utilized Sentinel-2 MultiSpectral Instrument (MSI) data acquired from the European Space Agency (ESA) to classify forest vegetation and assess changes within the Central Highlands and Southeast regions of Vietnam, covering the period from 2016–2024 (Table 1).

Sentinel-2 MSI (Level-2A surface reflectance) data were selected for their 10–20 m spatial resolution and the availability of Red Edge and SWIR bands, which improve discrimination of diverse tropical forest types across complex terrain. We used cloud-reduced dry-season composites for four target years (2016, 2020, 2021, and 2024). These years were chosen to align with national forest inventory cycles and reporting milestones to maximize policy relevance. In addition, high-quality Sentinel-2 L2A products with low cloud cover were available for the study area (Table 1). The timeline includes an initial baseline (2016), an intermediate phase covering pre- and post-policy/land-use changes (2020 and 2021), and the most recent map (2024) to capture short- and medium-term dynamics. Using dry-season composites (specifically images from around July for consistency) reduces phenological variability and improves interannual comparability.

Images were selected on the basis of minimal cloud cover and optimal image quality for each target year, including 2016, 2020, 2021 and 2024. These selection processes were performed via the Google Earth Engine (GEE) cloud computing platform, which enables efficient access and processing of a large volume of Sentinel-2 data.

The Sentinel-2 image data were preprocessed via the following steps:

- Atmospheric Correction: The Sen2Cor algorithm within the Sentinel application platform (SNAP) was used to mitigate atmospheric effects (absorption and scattering) and convert top-of-atmosphere reflectance values to surface reflectance values, increasing the accuracy of subsequent classification procedures.

- Spatial Subset (Clipping): Sentinel-2 images were spatially clipped to the boundaries of the study area to minimize data storage requirements and processing times.

- Vegetation Index Calculation: Standardized vegetation indices, including the normalized difference vegetation index (NDVI) and enhanced vegetation index (EVI), were calculated from Sentinel-2 spectral bands. The formulations for the NDVI and EVI calculations are as Eq. (1) (Rouse et al. 1974, Tucker 1979):

$$EVI = 2.5 \times \frac{R_{nir} - R_r}{R_{nir} + C1 \times R_r - C2 \times R_b + L} \quad (1)$$

Where R_b, R_r, and R_{nir} refer to the spectral reflectance values in the blue, red, and near-infrared bands, respectively.

C1 and *C2* are atmospheric correction coefficients (typically 6 and 7.5, respectively) designed to account for aerosol scattering in the red and blue bands, minimizing atmospheric influence and improving the linearity of the EVI signal.

L is a canopy background adjustment factor (typically 1) used to decouple soil background reflectance from the vegetation signal, particularly in areas with sparse canopy or varying soil conditions.

For Sentinel-2 images, the coefficients *C1*, *C2*, and L are set to the widely adopted standard values of 6, 7.5, and 1, respectively, as recommended for optimal EVI performance across various sensors (Huete et al. 2011).

Methods

Vegetation classification

Leveraging Sentinel-2 imagery and ancillary datasets, this study utilized the robust and effective RF algorithm, a supervised machine learning technique, for forest type classification (Breiman 2001). The overall classification process involved careful feature selection, systematic training sample collection, robust model training and optimization, and thorough accuracy assessment as detailed below.

Feature selection

The input feature set included spectral bands from Sentinel-2 images (B2, B3, B4, B8, B11, and B12), vegetation indices (NDVI and EVI), and terrain variables (slope, slope direction, and elevation). The selection of these features was based on their theoretical capacity to distinguish different types of vegetation in the study area, as well as insights gained from prior studies.

Training sample collection

Training samples were collected to represent the main vegetation types in the study area, such as tropical evergreen closed forests, deciduous open forests, plantations, and bare land (Fig. 2). The sources for sample collection included field surveys, high-resolution satellite imagery, and expert knowledge. A total of 12,000 reference samples were meticulously digitized. These samples were then proportionally allocated to individual classes based on their prevalence and distinctiveness. For example, Rich primary evergreen broadleaved forest (TXG1) had 209 samples, while croplands (NN) had 61 samples in 2024.

Table 1. Sentinel-2 satellite image parameters at the time of image collection

Year	Collection ID	Compositing Period	Platform	Cloud cover (%)	Season	Cloud-mask method	Bands
2016	COPERNICUS/S2_SR (L2A)	Dry Season Composite and July 2016	S2A	<10	Dry Season	QA60 bitmask	B2;B3;B4;B5;B6;B7;B8; B8A;B11;B12
2020	COPERNICUS/S2_SR (L2A)	Dry Season Composite and July 2020	S2B	<5	Dry Season	SCL cloud/shadow mask	B2;B3;B4;B5;B6;B7;B8; B8A;B11;B12
2021	COPERNICUS/S2_SR (L2A)	Dry Season Composite and July 2021	S2B	<5	Dry Season	SCL cloud/shadow mask	B2;B3;B4;B5;B6;B7;B8; B8A;B11;B12
2024	COPERNICUS/S2_SR (L2A)	Dry Season Composite and July 2024	S2B	<2	Dry Season	QA60 + SCL + BRDF mask	B2;B3;B4;B5;B6;B7;B8; B8A;B11;B12

Bands 5, 6, 7, 8A, 11, and 12 are 20 m; Bands 1, 9, and 10 are 60 m.

These samples were spatially distributed across the study area to ensure representativeness of various conditions and vegetation heterogeneity, as visually depicted in Fig. 2. From this total, 2100 samples (70%) were randomly selected for model training, and the remaining 900 samples (30%) were reserved as an independent test set for accuracy assessment (Table 2).

Random forest model training and classification

The RF model was trained using the 70% training data, implemented using the scikit-learn library in Python. To optimize the Random Forest model for robust vegetation classification, a systematic hyperparameter tuning process was conducted. Key hyperparameters, n_estimators (number of trees) and max_features (number of features considered at each split), were thoroughly evaluated. A range of values was tested: n_estimators (100, 200, 500, 1000) and max_features (from 1 to 10 with a step size of 1). Initial tests indicated that model stability and performance convergence primarily occurred when n_estimators ranged from 400 to 500. Consequently, n_estimators = 500 was chosen as the optimal value, balancing computational efficiency with predictive accuracy.

For max_features, testing across the specified range revealed that values of 2, 3, or 4 consistently yielded the highest classification performance. Detailed evaluation using the validation set showed that max_features = 3

Table 2. Number of sample points over time

№	Symbol	Types of forests	2016		2020		2021		2024	
			T	R	T	R	T	R	T	R
1	TXG1	Rich primary evergreen broadleaved forest	173	74	157	67	149	64	146	63
2	TXB1	Medium primary evergreen broadleaved forest	179	77	189	81	169	72	179	75
3	TXG	Rich secondary evergreen broadleaved forest	101	43	168	72	165	71	167	72
4	TXB	Medium secondary evergreen broadleaved forest	167	72	154	66	147	63	146	63
5	TXN	Poor secondary evergreen broadleaved forest	140	60	384	165	214	92	136	58
6	TXK	Very poor secondary evergreen broadleaved forest	155	66	79	34	118	51	102	44
7	TXP	Rehabilitation secondary evergreen broadleaved forest	140	60	141	60	55	24	85	36
8	RLG	Secondary deciduous forest	67	29	50	21	129	55	126	54
9	TXDG	Rich secondary coniferous forest	69	30	92	39	42	18	37	16
10	LKB	Medium secondary coniferous forest	70	30	160	69	66	28	67	29
11	RND	Secondary evergreen broadleaved forest on rocky mountain	118	51	66	28	106	45	304	130
12	RKG	Mixed wood-coniferous forest	55	24	64	27	150	64	126	54
13	RNMG	Mangrove forest	81	35	16	7	95	41	60	26
14	TLU	Bamboo forest	164	70	5	2	43	18	34	15
15	HG1	Mixed wood-bamboo forest	93	40	141	60	154	66	30	13
16	CDD	Palm and coconut tree forest	99	42	89	38	82	35	153	66
17	RTG	Timber plantation	55	24	38	16	54	24	75	32
18	DT2	Grasslands, shrubs, regenerated trees	45	19	31	15	45	19	39	17
19	NN	Crop lands	54	23	32	14	52	22	43	18
20	MN	Water bodies	34	15	20	9	33	14	22	9
21	DK	Other lands	41	16	24	10	32	14	23	10
Total			2100	900	2100	900	2100	900	2100	900
Overall accuracy			88.55		90.02		89.63		90.53	

Note: T = Training samples; R = Remaining samples.

achieved the highest overall accuracy (OA) of 90.53%, outperforming max_features = 2 (OA = 89.2%) and max_features = 4 (OA = 88.8%). Therefore, the final Random Forest classifier was configured with n_estimators = 500, max_features = 3, max_depth = None, min_samples_leaf = 1, and random_state = 42. After training, the optimized RF model was applied to the Sentinel-2 imagery for each target year (2016, 2020, 2021, 2024) to generate classified vegetation maps.

To assess forest change, vegetation classification maps from 2016, 2020, 2021, and 2024 were compared using a "pixel-based change detection" approach within ArcGIS, identifying deforestation, reforestation, and vegetation type conversion. The selection of these specific years (2016, 2020, 2021, and 2024) was primarily driven by their alignment with national forest inventory cycles and mandated project reporting milestones, ensuring the direct relevance and applicability of our findings for national forest management and policy.

Accuracy assessment

The accuracy of the land cover classification was assessed via precision, recall, and F1-scores for each class (Liang 2022). The F1 score provides a key metric for evaluating classification model performance, particularly in datasets with imbalanced class distributions. It reflects the harmonic mean of precision and recall, providing a comprehensive measure of the model's ability to both minimize false positives and correctly identify pixels belonging to each land cover class.

Precision, which represents the proportion of pixels correctly classified into a specific class out of all the pixels predicted to belong to that class, was calculated as Eq. (2):

$$Precision = \frac{TP}{TP + FP} \tag{2}$$

where true positive (TP) denotes the number of samples correctly classified as belonging to their respective class; false positive (FP) represents the number of samples incorrectly classified as belonging to a given class; and false negative (FN) indicates the number of samples that belong to a given class but are misclassified as belonging to another class.

Recall, also known as sensitivity, quantifies the model's ability to correctly identify all pixels belonging to a particular class and is defined as Eq. (3):

$$Recall = \frac{TP}{TP + FN} \tag{3}$$

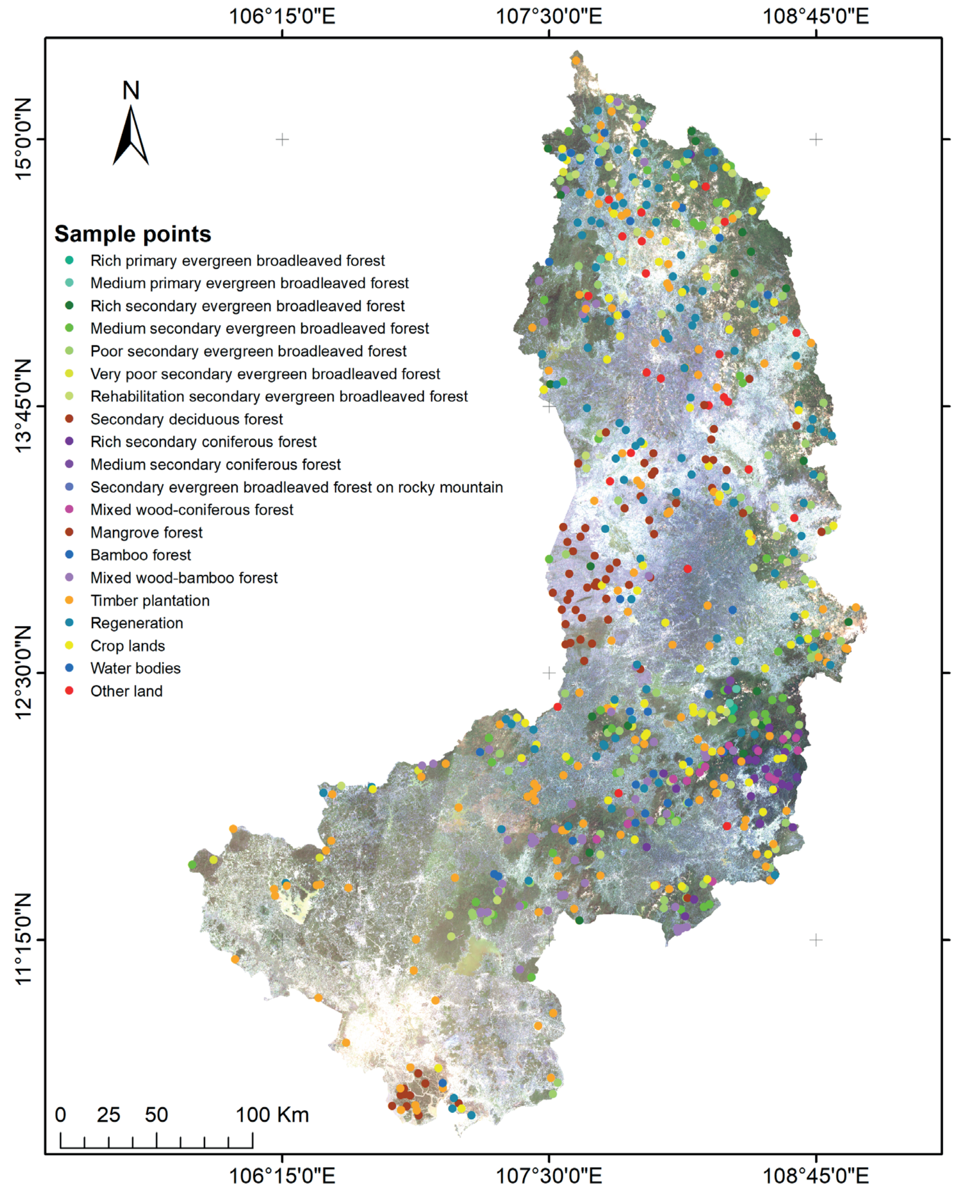

Fig. 2. Classification samples in the study area

The F1 score, which balances precision and recall, was computed via the following Eq. (4):

$$F1\ score = 2\frac{precision \times recall}{precision + recall} \tag{4}$$

This metric ensures that a high F1 score is achieved only when both precision and recall are high, providing a more robust assessment of classification performance. The F1 score ranges from 0 to 1, with a value of 1 representing perfect classification accuracy.

Vegetation Change Assessment

To assess the changes in forest vegetation from 2016 to 2024, we employed a pixel-based post-classification comparison method. This approach involves the sequential comparison of independently generated vegetation classification maps for each target year (2016, 2020, 2021, and 2024). Specifically, we overlaid pairs of classification maps representing consecutive periods, such as 2016–2020, 2020–2021, and 2021–2024, using ArcGIS software. By analyzing the transition matrix generated from these overlays, we identified three primary types of vegetation change:

Deforestation: This refers to the conversion of any type of "forest" (e.g., tropical evergreen closed forest, deciduous dipterocarp forest, timber plantations) to any type of "non-forest" (e.g., agricultural land, bare land, built-up areas, water bodies).

Forest restoration: This is the transition from any type of "non-forest" to any type of "forest."

Vegetation type transition: This describes the change between different types of "forest" (e.g., from tropical evergreen closed forest to deciduous dipterocarp forest) or between different types of "non-forest."

Pixels that maintained their original classification throughout the study period were categorized as "unchanged." This comprehensive method enables us to quantify the total area change and identify specific land use transitions and their geographical locations, offering detailed insights into the drivers and impacts of vegetation dynamics.

RESULTS

Forest types

In this study, the vegetation and land cover classification process identified 21 distinct classes across Vietnam's Central Highlands and Southeast regions. These classes were selected based on their structural, compositional, ecological roles, and management objectives, allowing for a comprehensive assessment of the diverse vegetation within the area. The main classified and compared classes include the following:

Natural forest types: This category encompasses various forms of evergreen broadleaf forests (e.g., Rich primary evergreen broadleaf forest – TXG1, Medium secondary evergreen broadleaf forest – TXB, Poor secondary evergreen broadleaf forest – TXN, etc.), secondary coniferous forests (TXDG, LKB), secondary deciduous forests (RLG), mixed wood-coniferous forests (RKG), mixed wood-bamboo forests (HG1), mangrove forests (RNMG), and bamboo forests (TLU).

Plantation forest types: this category primarily includes timber plantations (RTG) and palm/coconut tree forests (CDD).

Other vegetation and non-forest land: this group covers grasslands, shrubs, regenerated trees (DT2), crop lands (NN), water bodies (MN), and other land (DK).

A complete list of these classes and their corresponding symbols are detailed in Table 2 and the legend of Fig. 2.

Classification accuracy

The accuracy of the vegetation classification map was evaluated using the precision, recall, and F1 score metrics detailed in the methods section (Eqs. 2–4). Table 3 presents the accuracy assessment results for the 2024 classification map, offering a comprehensive overview of the classification performance.

The accuracy assessment revealed that forest types with distinct spectral characteristics were classified with high accuracy. For example, mangrove forest, timber plantation, and deciduous broadleaf forest showed elevated F1 score values (0.93, 0.90, and 0.87, respectively), demonstrating the model's ability to effectively discriminate these land cover types on the basis of their unique spectral signatures. In contrast, lower accuracy was observed for more complex forest types or those exhibiting spectral overlap with other land use categories. Rich evergreen broadleaf forest and palm forest, for example, yielded lower F1 score values (0.55 and 0.56, respectively), indicating challenges in distinguishing these classes owing to the inherent variability in forest structure, spectral confusion, or potentially nonrepresentative training samples.

Furthermore, an imbalance between precision and recall was observed for certain forest types, with rich evergreen broadleaf forests exhibiting low recall (0.46) and relatively high precision (0.70). This suggests that while the model demonstrates high confidence when classifying pixels as Rich evergreen broadleaf forests, it tends to omit pixels belonging to this class. These results indicate that the random forest algorithm generally performed well in classifying forest vegetation within the study area, but further refinements are needed to improve accuracy for complex forest types or those with significant spectral overlap with other land use categories.

The comparison of classification performance across different categories shows that classes with distinct spectral signatures and enough reference samples, such as mangrove forests, plantations, and secondary deciduous forests, were classified more accurately. In contrast, classes that exhibited high structural variability or spectral confusion, like several semi-natural evergreen broadleaf types and palm/coconut stands, were classified less reliably. The model appeared to be conservative for some high-value classes, particularly TXG, which resulted in high precision but low recall. This suggests that many true pixels were not classified—likely due to within-class heterogeneity or insufficient training samples that represent these classes adequately. Key sources of confusion include classes with similar structures or those located in transitional zones (which lead to mixed pixels), as well as areas with complex topography that create issues with illumination and shadow effects.

These observations highlight two main avenues for improvement: (1) targeted augmentation of training samples for underperforming classes, which should include additional field observations and high-resolution image analysis in boundary areas, and (2) the incorporation of complementary data, such as LiDAR, multi-temporal Sentinel-2 time series, or other spectral indices, to improve the discrimination among spectrally similar classes.

Table 3. Accuracy assessment results for the Central Highlands and Southeast Region

№	Symbol	Types of forests	Precision	Recall	F1 Score
1	TXG1	Rich primary evergreen broadleaved forest	0.74	0.65	0.69
2	TXB1	Medium primary evergreen broadleaved forest	0.85	0.82	0.84
3	TXG	Rich secondary evergreen broadleaved forest	0.70	0.46	0.55
4	TXB	Medium secondary evergreen broadleaved forest	0.86	0.89	0.88
5	TXN	Poor secondary evergreen broadleaved forest	0.76	0.73	0.74
6	TXK	Very poor secondary evergreen broadleaved forest	0.75	0.71	0.73
7	TXP	Rehabilitation secondary evergreen broadleaved forest	0.87	0.89	0.88
8	RLG	Secondary deciduous forest	0.88	0.86	0.89
9	TXDG	Rich secondary coniferous forest	0.74	0.69	0.72
10	LKB	Medium secondary coniferous forest	0.81	0.78	0.80
11	RND	Secondary evergreen broadleaved forest on rocky mountain	0.87	0.84	0.85
12	RKG	Mixed wood-coniferous forest	0.74	0.76	0.75
13	RNMG	Mangrove forest	0.91	0.90	0.93
14	TLU	Bamboo forest	0.88	0.89	0.86
15	HG1	Mixed wood-bamboo forest	0.82	0.84	0.83
16	CDD	Palm and coconut tree forest	0.62	0.51	0.56
17	RTG	Timber plantation	0.88	0.92	0.9
18	DT2	Grasslands, shrubs, regenerated trees	0.73	0.67	0.7
19	NN	Crop lands	0.85	0.82	0.84
20	MN	Water bodies	0.82	0.77	0.79
21	DK	Other lands	0.87	0.89	0.88
Average			0.81	0.78	0.79

Spectral characteristics of vegetation classes

On the basis of the accuracy assessment results, the reflectance spectral characteristics of different land cover types within the Central Highlands and Southeast regions of Vietnam were analyzed (Figs. 3–5).

Compared with non-forested land cover (e.g., other land and agriculture), natural forest types (e.g., rocky montane forest and evergreen broadleaf forest) generally presented lower reflectance values in the blue (0.17–0.20), green (0.17–0.20), and red (0.14–0.18) spectral regions. This pattern reflects the strong absorption of incident radiation by chlorophyll and other photosynthetic pigments within the plant canopies (Zhang et al. 2023). In contrast, the near-infrared (NIR) spectral region, which is highly sensitive to differences in vegetation structure and the internal structure of the leaf, presented relatively high reflectance values for forest types (0.30–0.45), indicating healthy leaf cellular structure and high water content (Fig. 3).

The vegetation red edge (VRE) channels (VRE1, VRE2, VRE3, and VRE4), which are sensitive to subtle variations in leaf cellular structure and chlorophyll content, also exhibited significant differences among vegetation types (Fig. 4). The forest types characterized by dense canopies (e.g., evergreen broadleaf forest and mixed forest) generally presented relatively high reflectance values in the VRE channels, which was indicative of relatively high aboveground biomass and chlorophyll concentrations. Conversely, non-forested land cover types (e.g., other land, agriculture) presented lower reflectance values in these spectral regions.

Shortwave infrared (SWIR) channels (SWIR1 and SWIR2), which are sensitive to variations in foliar and soil moisture contents, likewise provide differentiation among vegetation types (Fig. 5). Denser forest canopies are generally characterized by lower reflectance values in the SWIR channels, reflecting higher LWC. In contrast, non-forested land cover types presented higher reflectance values in these regions.

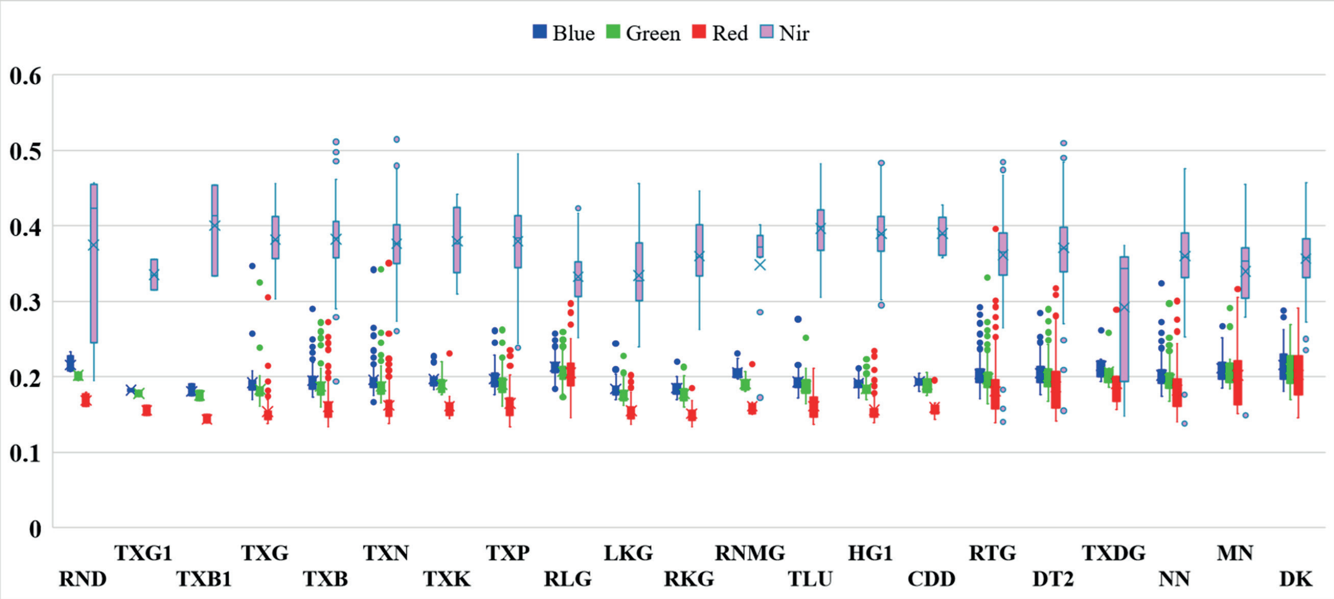

Fig. 3. Reflective spectral values of land cover types for four channels: blue, green, red, and NIR

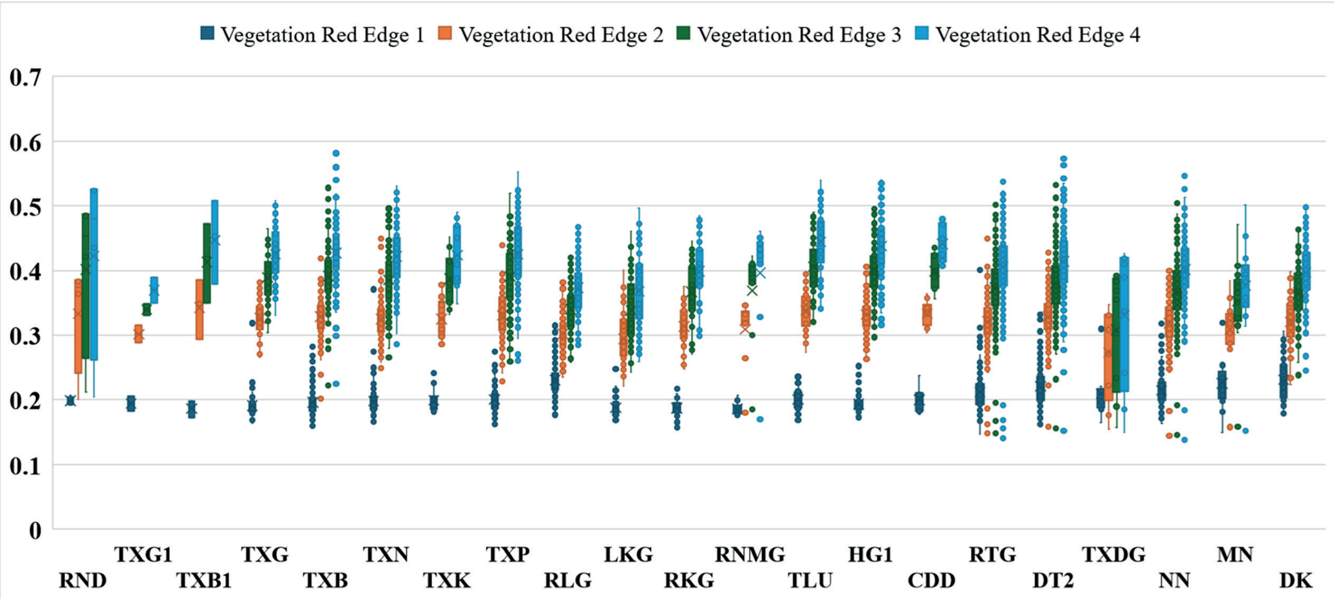

Fig. 4. Reflection spectral values of the overlay types for the four vegetation red edge spectral channels 1, 2, 3, and 4

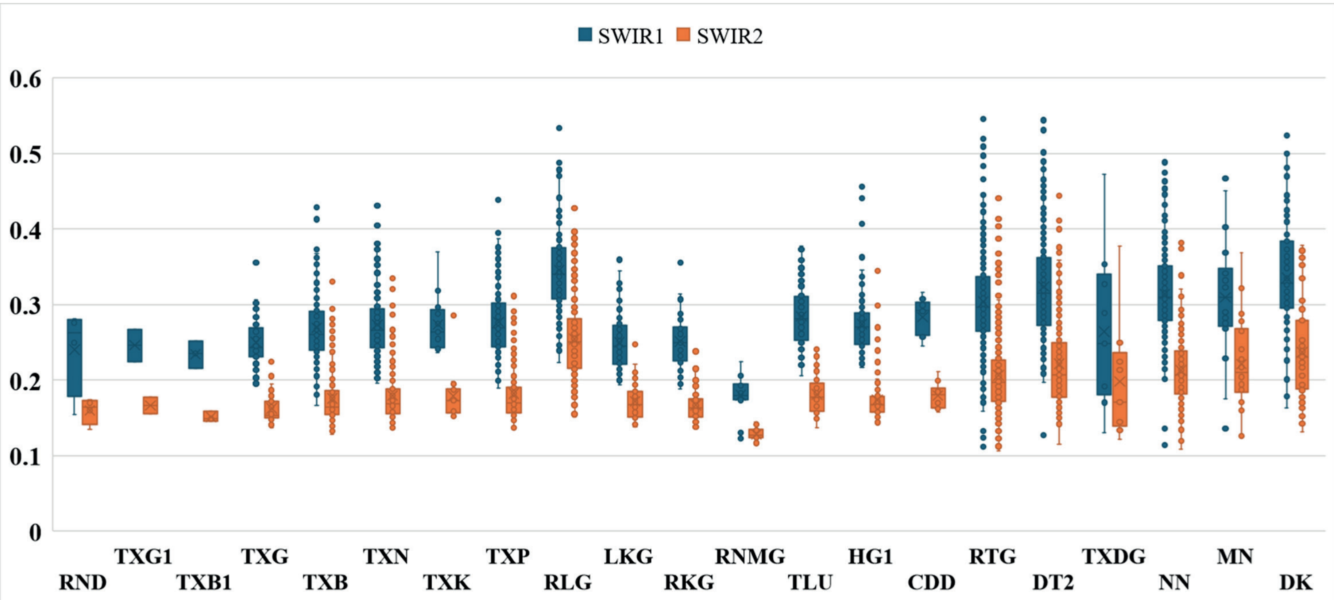

Fig. 5. Reflection spectral values of overlay types for 2 spectral channels, SWIR1 and SWIR2

Vegetation area and change

On the basis of the accuracy assessment, a map illustrating the current vegetation cover status for the Central Highlands and Southeast regions was created for 2016, 2020, 2021, and 2024 (Fig. 6). Table 4 presents the areas of the main vegetation types in the study area for these years.

According to the 2024 data (Table 4), the Central Highlands and Southeast regions maintain a diverse array of vegetation types, although some area changes have occurred since 2016.

Evergreen broadleaf forests represent the largest proportion, covering 665,792.3 hectares. These forests are predominantly situated within special-use forests (including national parks and nature reserves) and watershed protection areas, underscoring their significant ecological role in the region. Spatially, these evergreen broadleaf forests are primarily distributed across the eastern and northeastern parts of Gia Lai and Kon Tum provinces, extending into the southwestern section of Kon Tum province, the eastern areas of Dak Lak and Dak Nong provinces, and the northern reaches of Lam Dong province.

Timber plantations (RTG) also play an essential economic role, occupying 644,649.7 hectares. This forest type is widely distributed throughout the study area, stretching from the northern parts of Kon Tum province down to the southern extent in Ho Chi Minh City. Notably, the dominant species in timber plantations vary geographically: Acacia mangium is prevalent in the Central Highlands, whereas rubber *(Hevea brasiliensis)* plantations are more common in the Southeast region. Other natural forest types occupy smaller areas; for instance, poor evergreen broadleaf forests (TXN) cover 276,506.8 hectares. Deciduous broadleaf forests (RLG), a characteristic forest type of the Central Highlands, span 377,617.2 hectares and are primarily located in the western parts of Gia Lai and Dak Lak provinces.

Table 4. Current area of plant cover in the Central Highlands and Southeast region from 2016–2024

№	Symbol	Types of forests	Area (ha)			
			2016	2020	2021	2024
1	TXG1	Rich primary evergreen broadleaved forest	27,006	27,006	27,006	27,006
2	TXB1	Medium primary evergreen broadleaved forest	10,236	10,236	10,236	10,236
3	TXG	Rich secondary evergreen broadleaved forest	236,944	235,067	234,958	234,777
4	TXB	Medium secondary evergreen broadleaved forest	665,799	666,878	666,765	665,792
5	TXN	Poor secondary evergreen broadleaved forest	271,930	272,726	274,318	276,507
6	TXK	Very poor secondary evergreen broadleaved forest	18,771	18,172	17,539	17,330
7	TXP	Rehabilitation secondary evergreen broadleaved forest	300,209	297,005	296,869	299,504
8	RLG	Secondary deciduous forest	376,486	378,114	377,997	377,617
9	TXDG	Rich secondary coniferous forest	1,573	1,617	1,617	1,492
10	LKB	Medium secondary coniferous forest	116,299	117,388	117,292	115,611
11	RND	Secondary evergreen broadleaved forest on rocky mountain	5,797	7,875	7,875	7,813
12	RKG	Mixed wood-coniferous forest	49,963	50,164	50,070	48,858
13	RNMG	Mangrove forest	14,426	14,608	14,552	14,333
14	TLU	Bamboo forest	58,390	59,097	58,133	59,519
15	HG1	Mixed wood-bamboo forest	273,405	275,611	276,575	275,189
16	CDD	Palm and coconut tree forest	32	32	32	32
17	RTG	Timber plantation	644,330	646,664	646,301	644,650
18	DT2	Grasslands, shrubs, regenerated trees	340,816	330,958	330,547	329,524
19	NN	Crop lands	886,286	885,374	883,922	882,730
20	MN	Water bodies	45,025	44,844	44,900	45,119
21	DK	Other lands	3,442,932	3,447,222	3,449,153	3,452,664

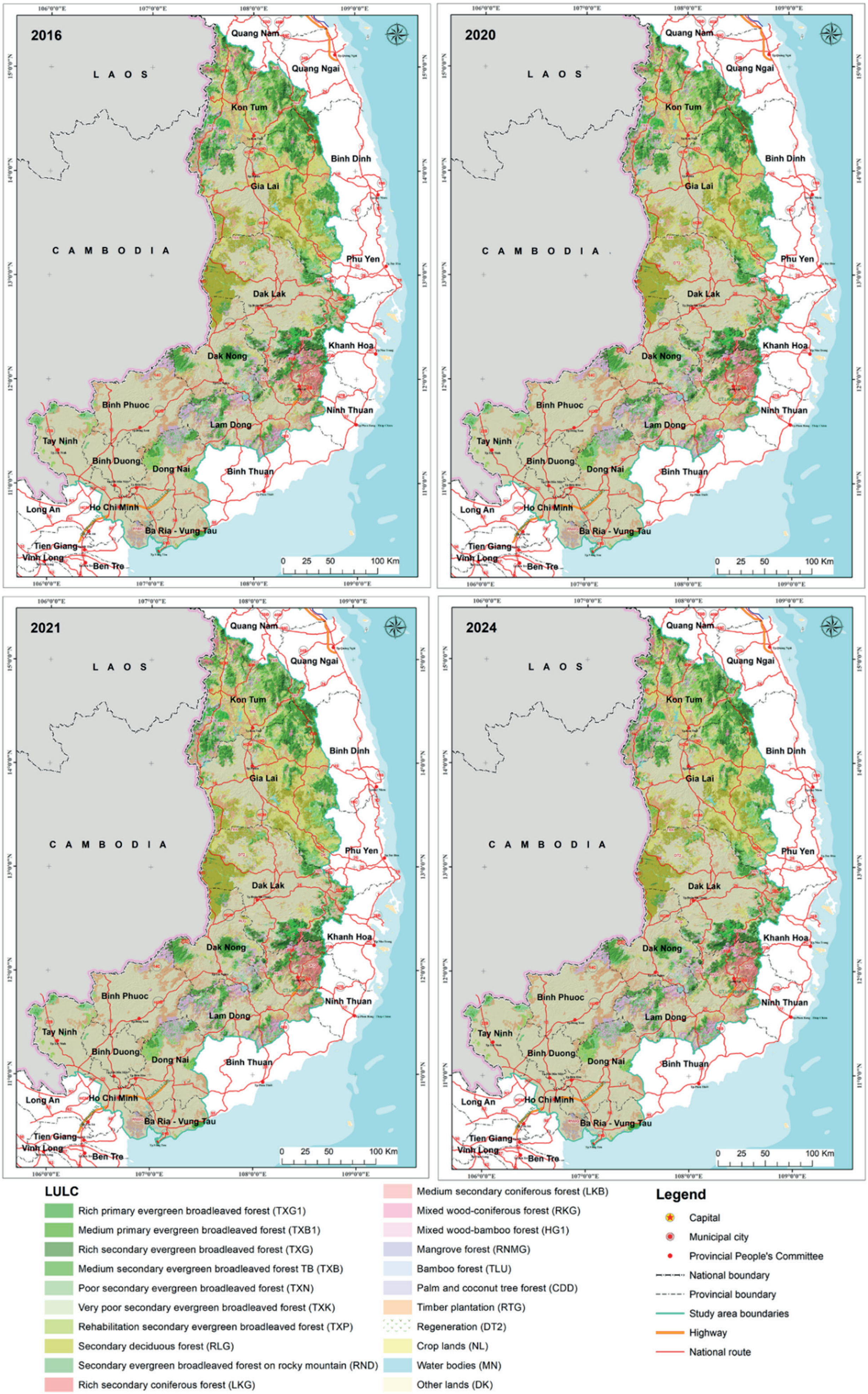

Fig. 6. Map of plant cover by period in the study area

Analysis of changes in the area of vegetation types from 2016–2024 revealed complex dynamics (Table 5). Certain vegetation types exhibit stability; for example, medium primary evergreen broadleaved forest maintained a consistent area of approximately 10,236 hectares throughout the study period, and palm and coconut tree forest remained stable at 32.2 hectares. This suggests the effectiveness of current conservation measures for these specific vegetation types.

However, area declines were noted for several natural forest types. The rich evergreen broadleaf forest area decreased from 236,943.6 hectares in 2016 to 234,777.1 hectares in 2024, a net reduction of 2,166.5 hectares. Declines are primarily located in the special-use forests and protective forests of the northern Central Highlands, including Chu Mom Ray, Kon Ka Kinh, Kon Chu Rang, and Thach Nham. The medium evergreen broadleaf forest area also experienced a slight decrease, from 665,799.2 hectares in 2016 to 665,792.3 hectares in 2024, representing a negligible reduction of 6.9 hectares. The areas of decline are similar to those of rich evergreen broadleaf forest. The area of poor evergreen broadleaf forest reportedly increased from 271,930.0 hectares in 2016 to 276,506.8 hectares in 2024. This shift was mainly due to the area of cropland, grassland, and shrubland in the study area. Overall, Rehabilitation Evergreen Broadleaf Forests showed some signs of recovery, decreasing from only 300,208.5 hectares in 2016 to 299,504.4 hectares in 2024. These declines indicate significant pressure on natural forests due to logging activities, land-use conversion, and other factors, including climate change and forest fires.

The area designated for timber plantation (RTG) initially increased from 644,329.9 hectares in 2016 to 646,663.9 hectares in 2020 but then slightly decreased to 644,649.7 hectares by 2024. This fluctuation may be attributed to the cyclical logging of plantations or their conversion to other land uses following harvest. Another noteworthy trend is the continuous increase in the area of other lands

Table 5. Transformation of plant cover areas in the Central Highlands and Southeast Vietnam from 2016–2024

№	Sym-bol	Types of forests	Area (increase (+)/decrease (-) (ha)		
			2020-2016	2021-2020	2024-2020
1	TXG1	Rich primary evergreen broadleaved forest	0.0	0.0	0.0
2	TXB1	Medium primary evergreen broadleaved forest	0.0	0.0	0.0
3	TXG	Rich secondary evergreen broadleaved forest	-1,877.1	-108.2	-181.2
4	TXB	Medium secondary evergreen broadleaved forest	1,078.6	-112.7	-972.8
5	TXN	Poor secondary evergreen broadleaved forest	796.2	1,592.0	2,188.6
6	TXK	Very poor secondary evergreen broadleaved forest	-600.2	-633.1	-209.0
7	TXP	Rehabilitation secondary evergreen broadleaved forest	-3,203.2	-136.1	2,635.1
9	RLG	Secondary deciduous forest	1,628.1	-116.5	-380.1
8	TXDG	Rich secondary coniferous forest	43.5	0.0	-124.8
10	LKB	Medium secondary coniferous forest	1,088.8	-96.1	-1,680.8
12	RND	Secondary evergreen broadleaved forest on rocky mountain	2,078.2	0.0	-62.0
11	RKG	Mixed wood-coniferous forest	201.0	-94.4	-1,211.4
13	RNMG	Mangrove forest	181.8	-56.1	-219.3
14	TLU	Bamboo forest	706.7	-964.0	1,385.8
15	HG1	Mixed wood-bamboo forest	2,206.0	964.0	-1,385.8
16	CDD	Palm and coconut tree forest	0.0	0.0	0.0
17	RTG	Timber plantation	2,334.1	-363.2	-1,651.0
18	DT2	Grasslands, shrubs, regenerated trees	-9,858.0	-411.4	-1,023.1
19	NN	Crop lands	-912.8	-1,451.4	-1,192.3
20	MN	Water bodies	-181.8	56.1	219.3
21	DK	Other lands	4,290.3	1,931.2	3,511.1

during the study period, which expanded from 3,442,931.9 hectares in 2016 to 3,452,664.4 hectares in 2024. This reflects the ongoing conversion of forestland to various other uses, including agricultural and construction land, which can have detrimental impacts on biodiversity, the ecological functions of forests, and the provision of ecosystem services.

Within the study area, forests within national parks and nature reserves exhibit relatively small fluctuations, partly due to the stable forest structure and effective management and protection efforts by local units. In contrast, the land cover types with the greatest area changes, such as grasslands, shrubs, and regenerated trees, are predominantly found in the buffer zones surrounding these national parks and nature reserves. The changes in various types of vegetation, particularly the decline in natural forest areas and the increase in non-forest land, highlight a complex interplay of ecological, socioeconomic, and policy factors. Certain forest types, such as evergreen broadleaf forests, appear more vulnerable to degradation, likely due to their structural weaknesses and direct human impacts. The rapid growth of "other lands" and "crop lands" indicates significant pressure on forest ecosystems.

Socioeconomic factors, including rising population density, the demand for agricultural land, and infrastructure development, directly influence these land-use changes. Economic incentives for converting forest land to agriculture or other uses often outweigh the benefits of preserving forest cover, particularly for local communities seeking to improve their livelihoods.

Policy frameworks also play a crucial role in shaping these dynamics. While forest protection and reforestation policies have led to some recovery—especially in planted forests—the continued decline in natural forests reveals gaps or challenges in policy implementation. The differing rates of decline observed between the 2016-2020 and 2021-2024 periods for natural forests suggest that recent policy adjustments or improved enforcement may be producing initial positive outcomes; however, further investigation is necessary. This situation underscores the need for adaptive management strategies that address both the direct and indirect drivers of deforestation and forest degradation, taking into account the specific ecological and socioeconomic contexts of different forest types.

DISCUSSION

Forest vegetation plays a critical role in maintaining ecological stability, conserving biodiversity, and providing essential ecosystem services (Brockerhoff et al. 2017, Wani et al. 2021). The Central Highlands and Southeast regions of Vietnam are home to diverse and ecologically significant forest ecosystems that contribute substantially to regional socioeconomic development and environmental protection (Cramb et al. 2004, Salemink 2018). This study provides a comprehensive assessment of the status and dynamics of forest vegetation in these regions from 2016–2024. The results of our vegetation classification indicate a diverse distribution of forest types, including tropical evergreen closed forests, deciduous dipterocarp forests, timber plantations, and non-forested land cover. However, analysis revealed a notable decline in the natural forest area during the study period.

The reflectance spectral characteristics of vegetation types are essential for accurate forest classification and monitoring. Natural forest types generally exhibit lower reflectance values in the blue, green, and red spectral bands because of the strong absorption of incident radiation by chlorophyll (do Amaral et al. 2019). Conversely, the near-infrared spectral region presents relatively high reflectance values for forest types, reflecting the leaf cellular structure and water content (Sims et al. 2002, Ullah et al. 2014). Vegetation red edge channels provide valuable information regarding vegetation health and physiological conditions (Shamsoddini et al. 2018), whereas SWIR channels are sensitive to variations in foliar and soil moisture content (Ullah et al. 2014). Integrating these spectral bands facilitates the accurate discrimination of diverse vegetation types and the monitoring of their temporal dynamics (Verrelst et al. 2019). Despite thorough preprocessing steps, which include atmospheric correction and cloud masking, remote sensing data still contains various types of noise. This noise can come from residual atmospheric effects, sensor-specific artifacts, and, notably, topographic variations in illumination, such as shadows and varying sun angles on slopes that are common in the mountainous Central Highlands. Such residual noise can significantly decrease the spectral separability between closely related vegetation types and contribute to mixed pixels. This, in turn, affects the overall accuracy and reliability of classification and change detection results. The lower F1 scores observed for certain complex forest types, such as rich evergreen broadleaf forests and coconut tree forests, may be partially due to these noise-induced spectral ambiguities, which complicate the precise delineation of class boundaries, even when using advanced machine learning algorithms.

Our change analysis reveals spatially heterogeneous losses and gains across the study area. At the class level, Rich secondary evergreen broadleaved forest experienced a net loss of 2,166.5 ha (2016–2024), while Medium secondary coniferous forest declined by 1,776.8 ha over the same period. These class-level changes are spatially concentrated: losses of high-value evergreen forests are primarily located in special-use and protection forest blocks in the northern Central Highlands (notably Chu Mom Ray, Kon Ka Kinh, Kon Chu Rang and Thach Nham). Compared with prior studies conducted in this region, our findings are consistent with reports of deforestation and forest degradation in the Central Highlands and Southeast regions (Khuc et al. 2018, Ebright et al. 2023). Prior studies have identified logging activities, land-use conversion, and agricultural expansion as the primary drivers of deforestation in this area (Meyfroidt et al. 2008, Meyfroidt et al. 2013, Tran et al. 2022). However, the present research provides more detailed quantitative evidence regarding the decline in area for specific forest types, as well as the expansion of nonforestland cover. Notably, the rate of natural forest decline slowed during the 2021–2024 period compared with the 2016–2020 period, potentially reflecting the effectiveness of conservation initiatives and/or the influence of broader climatic trends. Further research is warranted to elucidate the relative contributions of these factors. The timber plantation area showed short-term increase from 2016 to 2020 (+2,334.1 ha) followed by a modest decrease by 2024 (net +683.1 ha relative to 2016), consistent with harvest–replant cycles. The observed increase in timber plantation area from 2016–2020 indicates the initial success of afforestation programs; however, this area experienced a slight decrease from 2021–2024, likely due to timber harvesting or conversion to alternative land uses. This suggests the need for more effective and sustainable exploitation and management practices within timber plantation systems.

Both natural and anthropogenic factors influence vegetation dynamics within the study area. In addition to human impacts, natural factors such as climate (rainfall, temperature), topography (elevation, slope), and soil conditions also influence the distribution and development of different vegetation types (Zheng 2006, Dong et al. 2014, Asefa et al. 2020). Wildfires and disease outbreaks can also lead to significant forest degradation (Cobb et al. 2016). Anthropogenic influences, including illegal and unsustainable logging, land-use conversion (particularly for agriculture and urban development), and unsustainable farming practices, are major contributors to deforestation and forest degradation (Kyere-Boateng et al. 2021, Burgess et al. 2022). Furthermore, forest management policies can exert both positive and negative influences on vegetation dynamics (McCarthy et al. 2011, Choi et al. 2021).

A significant challenge in classifying forest vegetation in the study area arises from the seasonal spectral variations observed in semi-evergreen forests, which can result in misclassification (Mamnun et al. 2020). To tackle this issue, our methodology strategically employed Sentinel-2 imagery, primarily captured during the peak of the wet season in July for the respective study years (Mai Son et al. 2025). During this time, semi-evergreen vegetation is in its most vigorous growth phase, demonstrating optimal photosynthetic activity and a maximum leaf area index. This consistent phenology provides a more distinct and stable spectral signature, making it easier to differentiate from other types of vegetation. This targeted image acquisition strategy, complemented by ground validation, was essential for improving classification accuracy for these dynamic forest types, ultimately enhancing the reliability of our vegetation maps.

The Central Highlands and Southeast regions of Vietnam have significant potential for forest restoration across various landscape types. Degraded forest patches or buffer zones adjacent to relatively intact forest cores, such as areas converted from barren land, benefit from natural restoration due to local seed sources and connections to nearby protected areas. Plantation areas often exhibit rapid recovery cycles upon replanting, making it essential to prioritize the conversion to mixed native species to enhance biodiversity. Restoration priorities should be determined using a multi-criteria index that considers factors such as distance to primary forest, conversion time, threat level, socioeconomic feasibility, and landscape connectivity potential. On a practical level, initial priority actions include protecting areas from encroachment, supporting natural regeneration in marginal forest patches, and replanting native species in severely degraded areas. Monitoring the progress of recovery can be conducted continuously using Sentinel-2 satellites to analyze the NDVI/EVI index and cover change, in combination with field surveys to assess the quality of regeneration.

Limitations

This study demonstrated that integrating Sentinel-2 imagery with RF classification is highly effective for distinguishing different forest types. The 13 spectral bands of Sentinel-2, particularly the Red Edge and SWIR bands, are crucial for capturing changes in vegetation cover, leaf structure, and mesophyll scattering, which are essential for accurate classification in complex tropical ecosystems (Sibanda et al. 2019, E. D. Chaves et al. 2020). Additionally, using multi-temporal Sentinel-2 data enables the detection of changes over the study period, providing valuable insights into the dynamic processes of the forest (Hościło et al. 2019, Wakulińska et al. 2020). Third, although field data were utilized for model training and internal accuracy assessment, the comprehensive validation and independent verification of the resulting classification maps and change detection analyses with external field-collected ground truth data were not explicitly conducted. This limitation may introduce uncertainties regarding the absolute accuracy and generalizability of the findings, particularly in ecologically complex and heterogeneous landscapes.

However, the methodology of this study has certain limitations. While Sentinel-2 offers a favorable balance between spatial and temporal resolution, its pixel size of 10-20 meters for major swaths can be a limiting factor in accurately detecting small-scale deforestation events or complex forest changes, especially in highly fragmented areas (Grabska et al. 2020). Although the RF algorithm is powerful, it can sometimes struggle with spectral confusion between certain forest types, particularly those with overlapping spectral signatures or high structural variability (Chan et al. 2008).

Future research could explore integrating very high-resolution imagery or LiDAR data to capture finer spatial details (Singh et al. 2012), as well as experimenting with more advanced deep learning algorithms to potentially improve classification accuracy and address some of the spectral limitations encountered with RF in highly heterogeneous environments (Wang et al. 2021, He et al. 2023).

CONCLUSIONS

This study assessed the status and dynamics of forest vegetation in the Central Highlands and Southeast regions of Vietnam from 2016–2024. These regions are of substantial economic, social, and environmental importance to Vietnam. With the use of Sentinel-2 remote sensing data, advanced analytical techniques, and GIS tools, a detailed vegetation classification model and corresponding maps were developed to evaluate temporal changes in the areas of different forest types. The novelty of the study lies in integrating multi-year Sentinel-2 data (2016–2024) with an RF classification framework adapted for hilly terrain through the systematic design of a stratified training model and parameter optimization.

The primary findings revealed a notable decline in the area of natural forests, particularly those of high conservation value. These findings underscore the urgent need for sustainable forest management and biodiversity conservation initiatives in this region. Consequently, we recommend immediate, practical interventions, including stricter enforcement against illegal logging, expansion of community-based conservation programs, and strategic reforestation efforts focused on restoring degraded natural forest areas. This research provides timely and comprehensive information on the status and dynamics of forest vegetation while also identifying key drivers influencing these changes and assessing the effectiveness of existing forest management policies.

These findings can inform the development of more effective forest management strategies tailored to the specific socioeconomic and environmental contexts of the region. Given the growing impacts of climate change and increasing pressure on forest resources, the adoption of remote sensing and GIS technologies for systematic forest monitoring and adaptive management is crucial. Concerted action is urgently needed to protect these invaluable forest ecosystems for the benefit of current and future generations. The results provide practical recommendations on targeted protection, community-based restoration, and conversion of plantations to natural forests at hotspots and show that if current trends continue, managed plantations may recover to a modest extent while the loss of natural forests in buffer zones outside the protected area is likely to continue over the next decade.

REFERENCES

Amelung T., and Diehl M. (1992). Deforestation of tropical rainforests: economic causes and impact on development. Kiel, Tübingen: Institut für Weltwirtschaft, JCB Mohr (Paul Siebeck).

Aquilas N. A., Mukong A. K., Kimengsi J. N., and Ngangnchi F. H. (2022). Economic activities and deforestation in the Congo basin: An environmental kuznets curve framework analysis. Environmental Challenges:100553. DOI: 10.1016/j.envc.2022.100553.

Asefa M., Cao M., He Y., Mekonnen E., Song X., and Yang J. (2020). Ethiopian vegetation types, climate and topography. Plant Diversity:302-311. DOI: 10.1016/j.pld.2020.04.004.

Binswanger H. P. (1991). Brazilian policies that encourage deforestation in the Amazon. World Development:821-829. DOI: 10.1016/0305-750X(91)90135-5.

Breiman L. (2001). Random Forests. Machine Learning:5-32. DOI: 10.1023/A:1010933404324.

Brockerhoff E. G., Barbaro L., Castagneyrol B., Forrester D. I., Gardiner B., González-Olabarria J. R., Lyver P. O. B., Meurisse N., Oxbrough A., Taki H., Thompson I. D., Van Der Plas F., and Jactel H. (2017). Forest biodiversity, ecosystem functioning and the provision of ecosystem services. Biodiversity and Conservation:3005-3035. DOI: 10.1007/s10531-017-1453-2.

Burgess T. I., Oliva J., Sapsford S. J., Sakalidis M. L., Balocchi F., and Paap T. (2022). Anthropogenic Disturbances and the Emergence of Native Diseases: a Threat to Forest Health. Current Forestry Reports:111-123. DOI: 10.1007/s40725-022-00163-0.

Chan J. C.-W., and Paelinckx D. (2008). Evaluation of Random Forest and Adaboost tree-based ensemble classification and spectral band selection for ecotope mapping using airborne hyperspectral imagery. Remote Sensing of Environment:2999-3011. DOI: 10.1016/j.rse.2008.02.011.

Choi Y., Lim C.-H., Chung H. I., Kim Y., Cho H. J., Hwang J., Kraxner F., Biging G. S., Lee W.-K., Chon J., and Jeon S. W. (2021). Forest management can mitigate negative impacts of climate and land-use change on plant biodiversity: Insights from the Republic of Korea. Journal of Environmental Management:112400. DOI: 10.1016/j.jenvman.2021.112400.

Cobb R. C., Meentemeyer R. K., and Rizzo D. M. (2016). Wildfire and forest disease interaction lead to greater loss of soil nutrients and carbon. Oecologia:265-276. DOI: 10.1007/s00442-016-3649-7.

Cramb R. A., Purcell T., and Ho T. C. S. (2004). Participatory assessment of rural livelihoods in the Central Highlands of Vietnam. Agricultural Systems:255-272. DOI: 10.1016/j.agsy.2003.11.005.

Dennis R. A., Mayer J., Applegate G., Chokkalingam U., Colfer C. J. P., Kurniawan I., Lachowski H., Maus P., Permana R. P., Ruchiat Y., Stolle F., Suyanto, and Tomich T. P. (2005). Fire, People and Pixels: Linking Social Science and Remote Sensing to Understand Underlying Causes and Impacts of Fires in Indonesia. Human Ecology:465-504. DOI: 10.1007/s10745-005-5156-z.

Denslow J. S. (1987). Tropical Rainforest Gaps and Tree Species Diversity. Annual Review of Ecology and Systematics:431-451.

Dinh D. B., Ngo D. T., Nguyen H. D., Viet Nguyen H. H., and Dang N. T. (2023). Free satellite image data application for monitoring land use cover changes in the kon ha nung plateau, vietnam. Heliyon. DOI: 10.1016/j.heliyon.2023.e12864.

Do Amaral E. S., Vieira Silva D., Dos Anjos L., Schilling A. C., Dalmolin Â. C., and Mielke M. S. (2019). Relationships between reflectance and absorbance chlorophyll indices with RGB (Red, Green, Blue) image components in seedlings of tropical tree species at nursery stage. New Forests:377-388. DOI: 10.1007/s11056-018-9662-4.

Do A. N. T., and Do T. a. T. (2025). The Vulnerability of Industrial Crops in Dak Nong Province, Vietnam: The Impact of Urbanization Using Sentinel-2 Satellite Imagery. International Journal of Environmental Research:120. DOI: 10.1007/s41742-025-00792-w.

Dong Y., Xiong D., Su Z. A., Li J., Yang D., Shi L., and Liu G. (2014). The distribution of and factors influencing the vegetation in a gully in the Dry-hot Valley of southwest China. CATENA:60-67. DOI: 10.1016/j.catena.2013.12.009.

E. D. Chaves M., C. A. Picoli M., and D. Sanches I. (2020). Recent Applications of Landsat 8/OLI and Sentinel-2/MSI for Land Use and Land Cover Mapping: A Systematic Review. Remote Sensing. pp 3062.

Ebright S. J., Stan A. B., Sâm H. V., and Fulé P. Z. (2023). Protected Areas Conserved Forests from Fire and Deforestation in Vietnam's Central Highlands from 2001 to 2020. Fire:164. DOI: 10.3390/fire6040164.

Erinjery J. J., Singh M., and Kent R. (2018). Mapping and assessment of vegetation types in the tropical rainforests of the Western Ghats using multispectral Sentinel-2 and SAR Sentinel-1 satellite imagery. Remote Sensing of Environment:345-354. DOI: 10.1016/j.rse.2018.07.006.

Ferreira M. P., Lotte R. G., D'elia F. V., Stamatopoulos C., Kim D.-H., and Benjamin A. R. (2021). Accurate mapping of Brazil nut trees (Bertholletia excelsa) in Amazonian forests using WorldView-3 satellite images and convolutional neural networks. Ecological Informatics:101302. DOI: 10.1016/j.ecoinf.2021.101302.

Gärtner P., Förster M., and Kleinschmit B. (2016). The benefit of synthetically generated RapidEye and Landsat 8 data fusion time series for riparian forest disturbance monitoring. Remote Sensing of Environment:237-247. DOI: 10.1016/j.rse.2016.01.028.

Ghazoul J., and Sheil D. (2010). Tropical rain forest ecology, diversity, and conservation. Oxford University Press, pp 516.

Grabska E., Hawryło P., and Socha J. (2020). Continuous Detection of Small-Scale Changes in Scots Pine Dominated Stands Using Dense Sentinel-2 Time Series. Remote Sensing. pp 1298.

He Y., Jia K., and Wei Z. (2023). Improvements in Forest Segmentation Accuracy Using a New Deep Learning Architecture and Data Augmentation Technique. Remote Sensing. pp 2412.

Himeur Y., Rimal B., Tiwary A., and Amira A. (2022). Using artificial intelligence and data fusion for environmental monitoring: A review and future perspectives. Information Fusion:44-75. DOI: 10.1016/j.inffus.2022.06.003.

Hościło A., and Lewandowska A. (2019). Mapping Forest Type and Tree Species on a Regional Scale Using Multi-Temporal Sentinel-2 Data. Remote Sensing. pp 929.

Hudak A. T., Evans J. S., and Stuart Smith A. M. (2009). LiDAR Utility for Natural Resource Managers. Remote Sensing:934-951. DOI: 10.3390/rs1040934.

Huete A., Didan K., Van Leeuwen W., Miura T., and Glenn E. (2011). MODIS Vegetation Indices. In: Ramachandran B, Justice CO, and Abrams MJ (eds) Land Remote Sensing and Global Environmental Change: NASA's Earth Observing System and the Science of ASTER and MODIS. Springer New York, New York, NY, pp 579-602. DOI: 10.1007/978-1-4419-6749-7_26.

Huong N. T. T., Quynh C. T. N., Dinh N. D., Hoai C. T., Hang P. T., Bao H. D., Son N. T., Dan L. Q., and Anh P. T. (2021). Estimating tropical forest stand volume using Sentinel-2A imagery. 2021 Second International Conference on Intelligent Data Science Technologies and Applications (IDSTA). pp 130-137

Jahromi M. N., Jahromi M. N., Zolghadr-Asli B., Pourghasemi H. R., and Alavipanah S. K. (2021). Google Earth Engine and Its Application in Forest Sciences. In: Shit PK, Pourghasemi HR, Das P, and Bhunia GS (eds) Spatial Modeling in Forest Resources Management : Rural Livelihood and Sustainable Development. Springer International Publishing, Cham, pp 629-649. DOI: 10.1007/978-3-030-56542-8_2.

Karan S. K., Samadder S. R., and Maiti S. K. (2016). Assessment of the capability of remote sensing and GIS techniques for monitoring reclamation success in coal mine degraded lands. Journal of Environmental Management:272-283. DOI: 10.1016/j.jenvman.2016.07.070.

Khuc Q. V., Tran B. Q., Meyfroidt P., and Paschke M. W. (2018). Drivers of deforestation and forest degradation in Vietnam: An exploratory analysis at the national level. Forest Policy and Economics:128-141. DOI: 10.1016/j.forpol.2018.02.004.

Koskinen J., Leinonen U., Vollrath A., Ortmann A., Lindquist E., D'annunzio R., Pekkarinen A., and Käyhkö N. (2019). Participatory mapping of forest plantations with Open Foris and Google Earth Engine. ISPRS Journal of Photogrammetry and Remote Sensing:63-74. DOI: 10.1016/j.isprsjprs.2018.12.011.

Kumar R., Kumar A., and Saikia P. (2022). Deforestation and Forests Degradation Impacts on the Environment. In: Singh VP, Yadav S, Yadav KK, and Yadava RN (eds) Environmental Degradation: Challenges and Strategies for Mitigation. Springer International Publishing, Cham, pp 19-46. DOI: 10.1007/978-3-030-95542-7_2.

Kyere-Boateng R., and Marek M. V. (2021). Analysis of the Social-Ecological Causes of Deforestation and Forest Degradation in Ghana: Application of the DPSIR Framework. Forests:409. DOI: 10.3390/f12040409.

Lechner A. M., Foody G. M., and Boyd D. S. (2020). Applications in Remote Sensing to Forest Ecology and Management. One Earth:405-412. DOI: 10.1016/j.oneear.2020.05.001.

Liang J. (2022). Confusion Matrix: Machine Learning. POGIL Activity Clearinghouse.

Lung N. N., Quat N. X., Lien A., Que A., Van Con A., Ky A., and Cam L. V. (2011). Final report on forest ecological stratification in Vietnam.

Luong N. V., Tateishi R., Hoan N. T., and Tu T. T. (2015). Forest change and its effect on biomass in Yok Don National Park in Central Highlands of Vietnam using ground data and geospatial techniques. Advances in Remote Sensing:108-118. DOI: 10.4236/ars.2015.42010.

Mai Son L., Nguyen Manh H., Dao Duy T., Tu Dinh D., Binh Tran T., and Le Dung T. K. (2025). Monitoring spatial-temporal dynamics of drought over Yok Don National Park using Temperature-soil Moisture Dryness Index (TMDI). Vietnam Journal of Earth Sciences:252-271. DOI: 10.15625/2615-9783/22704.

Mamnun M., and Hossen S. (2020). Spatio-temporal analysis of land cover changes in the evergreen and semi-evergreen rainforests: A case study in Chittagong Hill Tracts, Bangladesh. International Journal of Forestry, Ecology Environmental pollution:87-99. DOI: 10.18801/ijfee.020220.10.

Matricardi E. a. T., Skole D. L., Pedlowski M. A., Chomentowski W., and Fernandes L. C. (2010). Assessment of tropical forest degradation by selective logging and fire using Landsat imagery. Remote Sensing of Environment:1117-1129. DOI: 10.1016/j.rse.2010.01.001.

Mccarthy N., Bentsen N. S., Willoughby I., and Balandier P. (2011). The state of forest vegetation management in Europe in the 21st century. European Journal of Forest Research:7-16. DOI: 10.1007/s10342-010-0429-5.

Meyfroidt P., and Lambin E. F. (2008). The causes of the reforestation in Vietnam. Land Use Policy:182-197. DOI: 10.1016/j.landusepol.2007.06.001.

Meyfroidt P., Vu T. P., and Hoang V. A. (2013). Trajectories of deforestation, coffee expansion and displacement of shifting cultivation in the Central Highlands of Vietnam. Global Environmental Change:1187-1198. DOI: 10.1016/j.gloenvcha.2013.04.005.

Mujetahid A., Nursaputra M., and Soma A. S. (2023). Monitoring Illegal Logging Using Google Earth Engine in Sulawesi Selatan Tropical Forest, Indonesia. Forests:652. DOI: 10.3390/f14030652.

Ngo D. T., Quoc K. N., Dang N. T., Dang C. H., Tran L. L., and Nguyen H. D. (2024). Analysis Of The Mangrove Structure In The Dong Rui Commune Based On Multispectral Unmanned Aerial Vehicle Image Data. GEOGRAPHY, ENVIRONMENT, SUSTAINABILITY:14-25. DOI: 10.24057/2071-9388-2023-2641.

Nguyen Duc K., Ancev T., and Randall A. (2019). Evidence of climatic change in Vietnam: Some implications for agricultural production. Journal of Environmental Management:524-545. DOI: 10.1016/j.jenvman.2018.10.011.

Nguyen H. S., Khau T. L., and Huynh T. T. (2025). Investigation of Natural and Human-Induced Landslides in Red Basaltic Soils. Water:1320. DOI: 10.3390/w17091320.

Nguyen H. T., Doan T. M., Tomppo E., and Mcroberts R. E. (2020). Land Use/Land Cover Mapping Using Multitemporal Sentinel-2 Imagery and Four Classification Methods—A Case Study from Dak Nong, Vietnam. Remote Sensing.

Ogboi K. C. (2001). Deforestation of the Tropical RainForest and Its Impact on Climate Change. ournal of Environmental Management Safety:28-37.

Ostendorf B., Hilbert D. W., and Hopkins M. S. (2001). The effect of climate change on tropical rainforest vegetation pattern. Ecological Modelling:211-224. DOI: 10.1016/S0304-3800(01)00392-1.

Phalke A. R., Özdoğan M., Thenkabail P. S., Erickson T., Gorelick N., Yadav K., and Congalton R. G. (2020). Mapping croplands of Europe, Middle East, Russia, and Central Asia using Landsat, Random Forest, and Google Earth Engine. ISPRS Journal of Photogrammetry and Remote Sensing:104-122. DOI: 10.1016/j.isprsjprs.2020.06.022.

Pijanowski B. C., Brown D. G., Shellito B. A., and Manik G. A. (2002). Using neural networks and GIS to forecast land use changes: a Land Transformation Model. Computers, Environment and Urban Systems:553-575. DOI: 10.1016/S0198-9715(01)00015-1.

Raši R., Bodart C., Stibig H.-J., Eva H., Beuchle R., Carboni S., Simonetti D., and Achard F. (2011). An automated approach for segmenting and classifying a large sample of multi-date Landsat imagery for pan-tropical forest monitoring. Remote Sensing of Environment:3659-3669. DOI: 10.1016/j.rse.2011.09.004.

Reddy C. S., Singh S., Dadhwal V. K., Jha C. S., Rao N. R., and Diwakar P. G. (2017). Predictive modelling of the spatial pattern of past and future forest cover changes in India. Journal of Earth System Science:8. DOI: 10.1007/s12040-016-0786-7.

Rouse J., Haas R., Schell J., and Deering D. (1974). Monitoring Vegetation Systems in the Great Plains with ERTS. NASA Special Publication.

Saim A. A., and Aly M. H. (2025). Fusion-Based Approaches and Machine Learning Algorithms for Forest Monitoring: A Systematic Review. Wild:7. DOI: 10.3390/wild2010007.

Salemink O. (2018). The Regional Centrality of Vietnam's Central Highlands. Oxford University Press.

Schnell S., Kleinn C., and Ståhl G. (2015). Monitoring trees outside forests: a review. Environmental Monitoring and Assessment:600. DOI: 10.1007/s10661-015-4817-7.

Shamsoddini A., and Raval S. (2018). Mapping red edge-based vegetation health indicators using Landsat TM data for Australian native vegetation cover. Earth Science Informatics:545-552. DOI: 10.1007/s12145-018-0347-5.

Shinjo H., Le H. T. T., Funakawa S., and Shine T. (2024). Overview of Vietnam. In: Fujii S, Funakawa S, Kobayashi H, Saizen I, Harada H, Shinjo H, Huynh HT, Hoang H, Tran DT, Tran VQ, and Le AV (eds) Livelihood and the Environment in Vietnam. Springer Nature Singapore, Singapore, pp 11-30. DOI: 10.1007/978-981-97-2289-1_2.

Sibanda M., Mutanga O., Dube T., S Vundla T., and L Mafongoya P. (2019). Estimating LAI and mapping canopy storage capacity for hydrological applications in wattle infested ecosystems using Sentinel-2 MSI derived red edge bands. GIScience & Remote Sensing:68-86. DOI: 10.1080/15481603.2018.1492213.

Sims D. A., and Gamon J. A. (2002). Relationships between leaf pigment content and spectral reflectance across a wide range of species, leaf structures and developmental stages. Remote Sensing of Environment:337-354. DOI: 10.1016/S0034-4257(02)00010-X.

Singh K. K., Vogler J. B., Shoemaker D. A., and Meentemeyer R. K. (2012). LiDAR-Landsat data fusion for large-area assessment of urban land cover: Balancing spatial resolution, data volume and mapping accuracy. ISPRS Journal of Photogrammetry and Remote Sensing:110-121. DOI: 10.1016/j.isprsjprs.2012.09.009.

Sothe C., De Almeida C. M., Schimalski M. B., La Rosa L. E. C., Castro J. D. B., Feitosa R. Q., Dalponte M., Lima C. L., Liesenberg V., Miyoshi G. T., and Tommaselli A. M. G. (2020). Comparative performance of convolutional neural network, weighted and conventional support vector machine and random forest for classifying tree species using hyperspectral and photogrammetric data. GIScience & Remote Sensing:369-394. DOI: 10.1080/15481603.2020.1712102.

Sothe C., De Almeida C. M., Schimalski M. B., Liesenberg V., La Rosa L. E. C., Castro J. D. B., and Feitosa R. Q. (2020). A comparison of machine and deep-learning algorithms applied to multisource data for a subtropical forest area classification. International Journal of Remote Sensing:1943-1969. DOI: 10.1080/01431161.2019.1681600.

Tai V. A., Thi Thuy Van T., Quang Tuan B., and Duc Hoang L. (2021). Ecological Characteristic of Grazing Vegetation and Capacity Food for the Large Cattle in Central Highland, Vietnam. VNU Journal of Science: Earth and Environmental Sciences. DOI: 10.25073/2588-1094/vnuees.4528.

Thi Hoai C., Thi Thanh Huong N., and Thi Hong Diep N. (2025). Application of Sentinel-2A/B and Landsat 9 Imagery in Vegetation Cover Assessment: A Case Study in Dak Glong and Krong No Districts, Dak Nong Province. IOP Conference Series: Earth and Environmental Science:012010. DOI: 10.1088/1755-1315/1501/1/012010.

Tran D. X., Tran T. V., Pearson D., Myint S. W., Lowry J., and Nguyen T. T. (2022). Spatiotemporal analysis of forest cover change and associated environmental challenges: a case study in the Central Highlands of Vietnam. Geocarto International:9277-9297. DOI: 10.1080/10106049.2021.2017013.

Tucker C. (1979). Red and Photographic Infrared Linear Combinations for Monitoring Vegetation. Remote Sensing of Environment. DOI: 10.1016/0034-4257(79)90013-0.

Turner E. C., and Snaddon J. L. (2023). Chapter 16 - Deforestation in Southeast Asia. In: Sivanpillai R, and Shroder JF (eds) Biological and Environmental Hazards, Risks, and Disasters (Second Edition). Elsevier, Boston, pp 319-334. DOI: 10.1016/B978-0-12-820509-9.00004-6.

Ullah S., Skidmore A. K., Ramoelo A., Groen T. A., Naeem M., and Ali A. (2014). Retrieval of leaf water content spanning the visible to thermal infrared spectra. ISPRS Journal of Photogrammetry and Remote Sensing:56-64. DOI: 10.1016/j.isprsjprs.2014.04.005.

Van Minh N., Hoang D. T., Van Loc N., and Long N. V. J. a. J. O. C. S. (2020). Effects of plant density on growth, yield and seed quality of quinoa genotypes under rain-fed conditions on red basalt soil regions. Australian Journal of Crop Science:1977-1982.

Verrelst J., Malenovský Z., Van Der Tol C., Camps-Valls G., Gastellu-Etchegorry J.-P., Lewis P., North P., and Moreno J. (2019). Quantifying Vegetation Biophysical Variables from Imaging Spectroscopy Data: A Review on Retrieval Methods. Surveys in Geophysics:589-629. DOI: 10.1007/s10712-018-9478-y.

Vu M. T., Raghavan S. V., Pham D. M., and Liong S.-Y. (2015). Investigating drought over the Central Highland, Vietnam, using regional climate models. Journal of Hydrology:265-273. DOI: 10.1016/j.jhydrol.2014.11.006.

Wakulińska M., and Marcinkowska-Ochtyra A. (2020). Multi-Temporal Sentinel-2 Data in Classification of Mountain Vegetation. Remote Sensing. pp 2696.

Wan Mahari W. A., Azwar E., Li Y., Wang Y., Peng W., Ma N. L., Yang H., Rinklebe J., Lam S. S., and Sonne C. (2020). Deforestation of rainforests requires active use of UN's Sustainable Development Goals. Science of The Total Environment:140681. DOI: 10.1016/j.scitotenv.2020.140681.

Wang T., Zuo Y., Manda T., Hwarari D., and Yang L. (2025). Harnessing Artificial Intelligence, Machine Learning and Deep Learning for Sustainable Forestry Management and Conservation: Transformative Potential and Future Perspectives. Plants:998. DOI: 10.3390/plants14070998.

Wang Y., Zhang W., Gao R., Jin Z., and Wang X. (2021). Recent advances in the application of deep learning methods to forestry. Wood Science and Technology:1171-1202. DOI: 10.1007/s00226-021-01309-2.

Wani A. M., and Sahoo G. (2021). Forest Ecosystem Services and Biodiversity. In: Shit PK, Pourghasemi HR, Das P, and Bhunia GS (eds) Spatial Modeling in Forest Resources Management : Rural Livelihood and Sustainable Development. Springer International Publishing, Cham, pp 529-552. DOI: 10.1007/978-3-030-56542-8_22.

Weiers S., Bock M., Wissen M., and Rossner G. (2004). Mapping and indicator approaches for the assessment of habitats at different scales using remote sensing and GIS methods. Landscape and Urban Planning:43-65. DOI: 10.1016/S0169-2046(03)00028-8.

Yun T., Li J., Ma L., Zhou J., Wang R., Eichhorn M. P., and Zhang H. (2024). Status, advancements and prospects of deep learning methods applied in forest studies. International Journal of Applied Earth Observation and Geoinformation:103938. DOI: 10.1016/j.jag.2024.103938.

Zhang S., Peng P., Bai M., Wang X., Zhang L., Hu J., Wang M., Wang X., Wang J., Zhang D., Sun X., and Dai X. (2023). Vegetation Subtype Classification of Evergreen Broad-Leaved Forests in Mountainous Areas Using a Hierarchy-Based Classifier. Remote Sensing.

Zheng F.-L. (2006). Effect of Vegetation Changes on Soil Erosion on the Loess Plateau1 1Project supported by the Chinese Academy of Sciences (No. KZCX3-SW-422) and the National Natural Science Foundation of China (Nos. 9032001 and 40335050). Pedosphere:420-427. DOI: 10.1016/S1002-0160(06)60071-4.